Cell Reports, Volume *39*

Supplemental information

Germinal center expansion but not plasmablast differentiation is proportional to peptide-MHCII density via CD40-CD40L signaling strength

Zhixin Jing, Mark J. McCarron, Michael L. Dustin, and David R. Fooksman

A

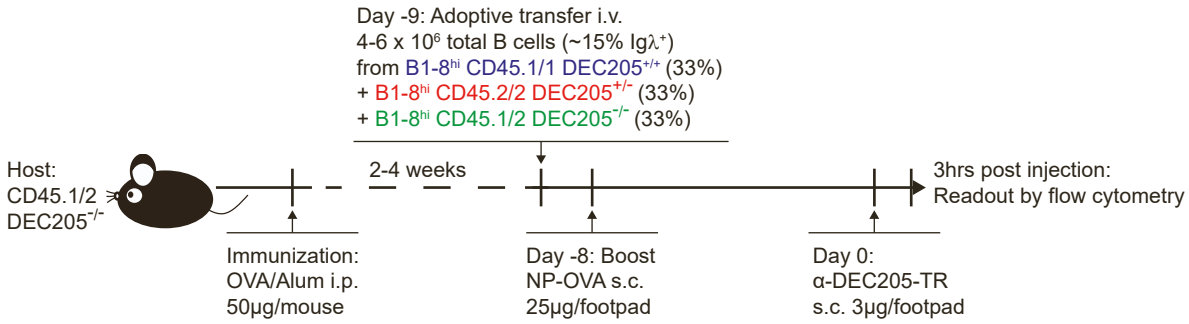

B

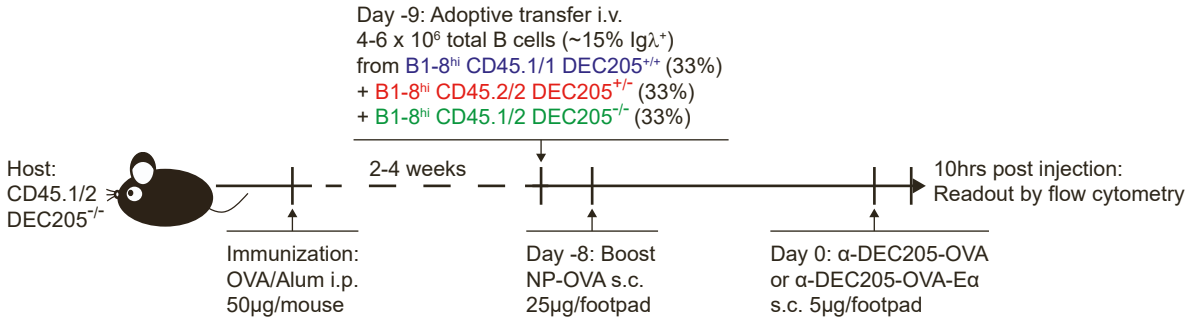

C

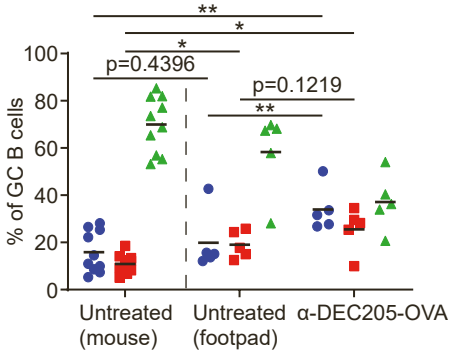

D

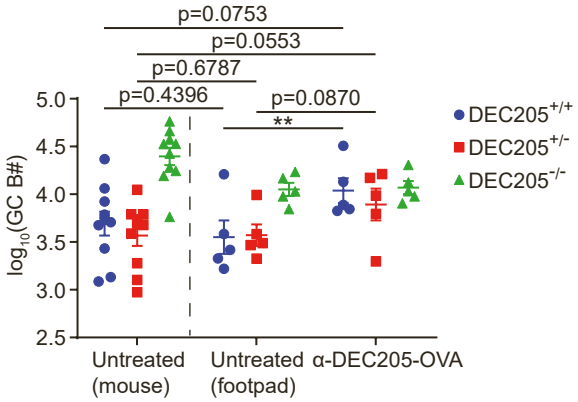

Supplemental Figure 1

Supplemental Figure 1. Differential pMHCII density can be controlled by αDEC-OVA targeting. Related to Figure 1.

(A), Experimental setup to examine antigen uptake level of GC B cells with differential DEC205 surface level by αDEC-Texas Red targeting. (B), Experimental setup to examine the level of cognate peptide presentation on MHCII of GC B cells with differential DEC205 surface level by αDEC-OVA-Eα targeting. (C), Frequency and (D), Log-transformed absolute numbers of GC B cells with differential pMHCII level conferred by αDEC-OVA targeting compared to contralateral untreated footpad of the same mouse or untreated footpad of control mice that received no treatment. All bars show mean (C) or mean ± SEM (D). *, $P < 0.05$; **, $P < 0.01$; exact p values, ns, non-significant by Mann Whitney U test (between treated mice to untreated mice) or paired Student's t test (between treated footpad and untreated footpad in the same mouse). All graphs show pooled data from at least two independent experiments. (C-D, n = 5-10)

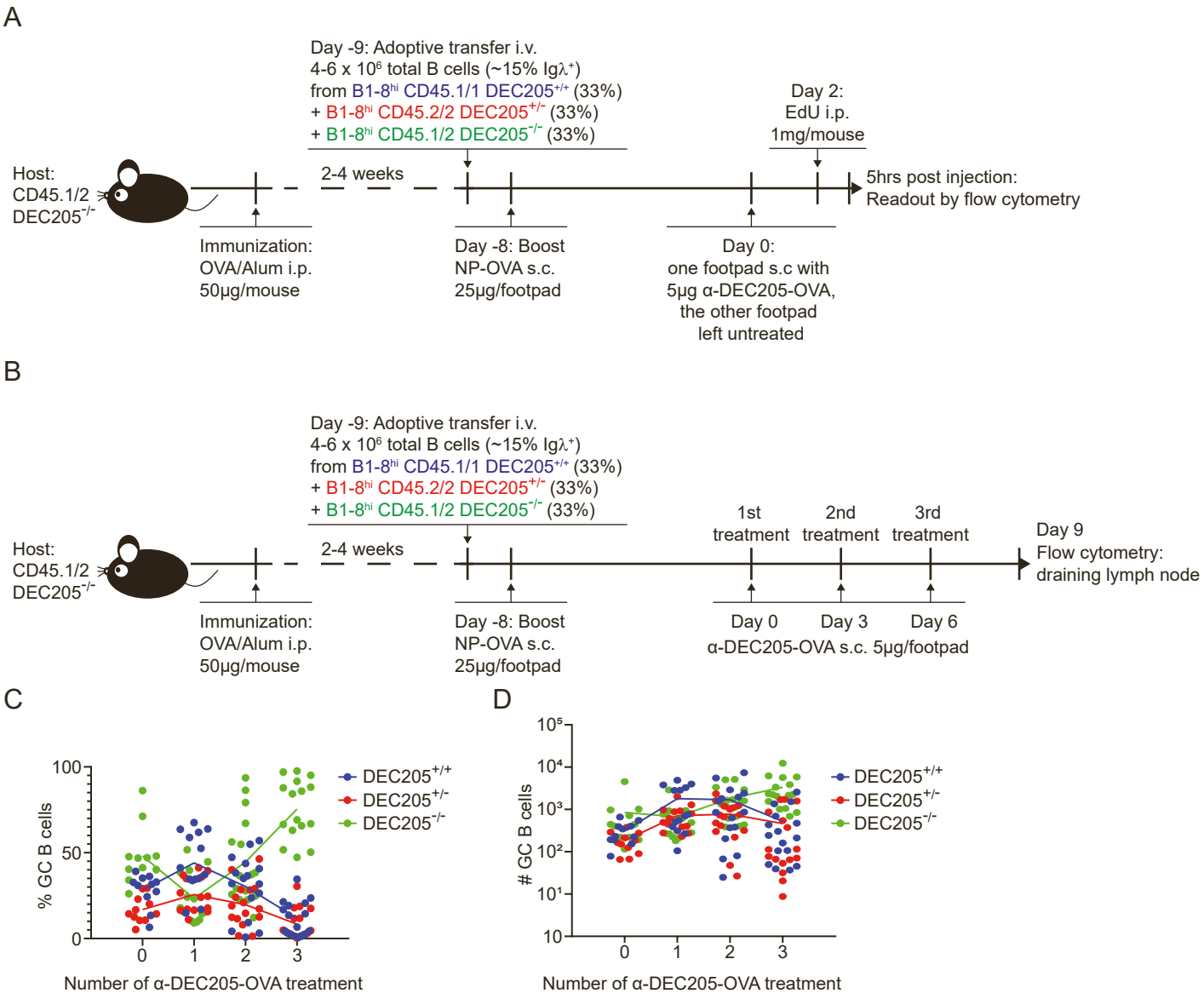

Supplemental Figure 2

Supplemental Figure 2. GC B cells with intermediate pMHCII density are not outcompeted by ones with high pMHCII density by multiple rounds of αDEC-OVA targeting. Related to Figure 2.

(A), Experimental setup for measuring EdU incorporation of GC B cells with differential pMHCII level conferred by αDEC-OVA targeting. (B), Experimental setup for direct competition of GC B cells with differential pMHCII density conferred by multiple αDEC-OVA targeting given every 3 days, each timepoint were analyzed by flow cytometry 3 days after the each αDEC-OVA treatment (i.e. Day 0, no treatment; Day 3, 1 treatment; Day 6, 2 treatments; Day 9, 3 treatments). (C), Kinetics of frequency and (D), absolute numbers of GC B cells with differential pMHCII level over multiple αDEC-OVA targeting. All graphs show pooled data from at least two independent experiments. (C-D, n = 11-16)

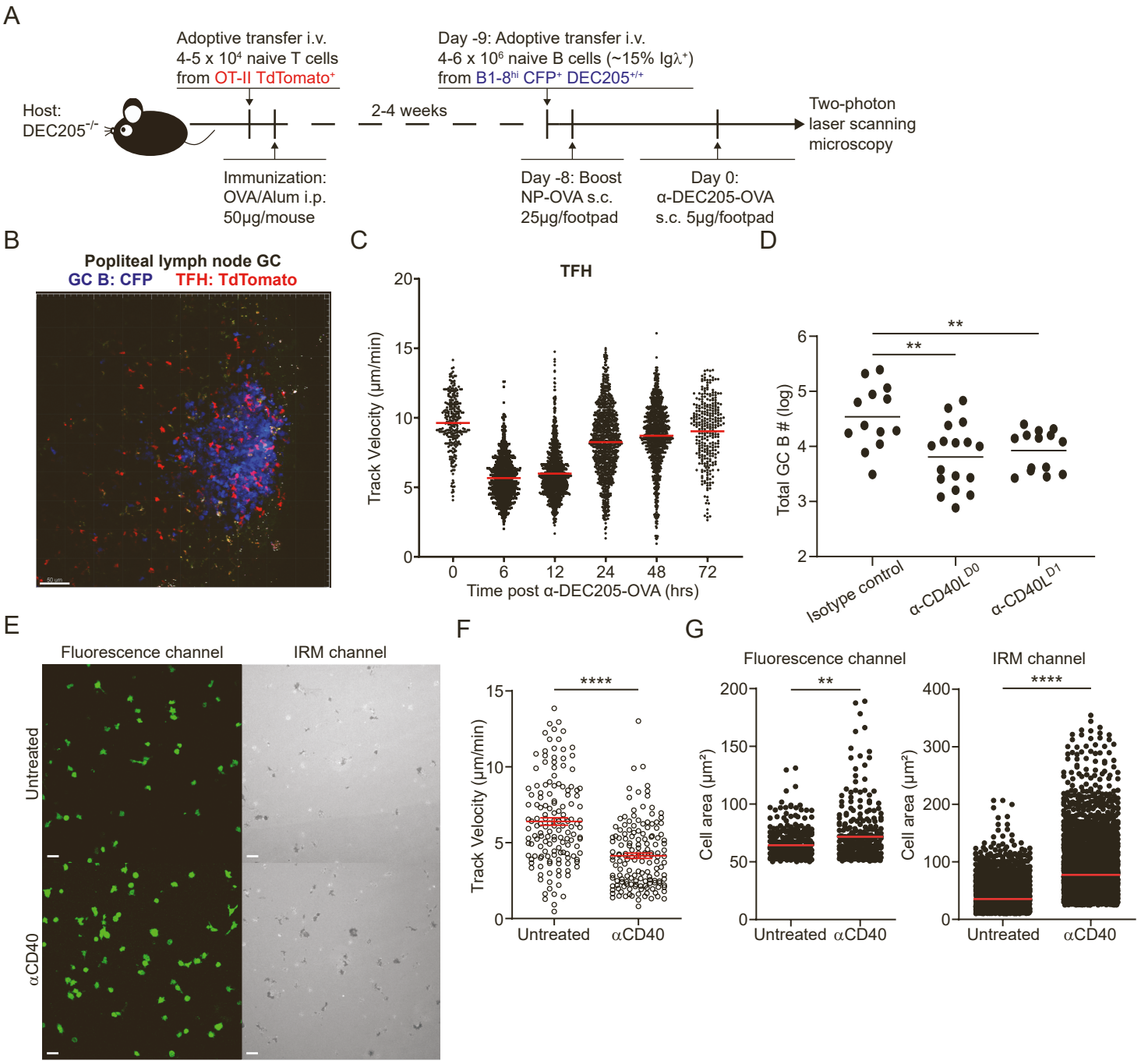

Supplemental Figure 3

Supplemental Figure 3. T cell help is temporarily delivered to GC B cells early after αDEC-OVA targeting. Related to Figure 3.

(A), Experimental setup for imaging kinetics of GC TFH and B cell dynamics post αDEC-OVA treatment by two-photon laser scanning microscopy. (B), Example of single timepoint snapshot of dynamics of TFH (red) and B cell (blue) interactions in the GC. Scale bar is 50μm. (C), Kinetics of TFH track velocity post αDEC-OVA treatment. (D) Log-transformed absolute numbers of total GC B cells in mice treated with isotype control antibody or neutralizing αCD40L at Day 0 or Day 1 after αDEC-OVA treatment. (E), Example of single timepoint snapshot of *in vitro* morphology and dynamics of GFP^+ B cell blasts (green) with or without agonist anti-CD40 by internal reflection microscopy (IRM). Scale bar is 30μm. (F), Track velocity and (G), Cell area under fluorescence channel and IRM channel of GFP^+ B cell blasts with or without agonist anti-CD40. All bars show mean (C,D, and G) or mean ± SEM (F). **, $P< 0.01$; ****, $P< 0.0001$ by Mann Whitney U test (F, and G) or unpaired Student's t test (D). All data are pooled data from (C and D) or representative of (F and G) at least two independent experiments. (C, n =2-3; D, n = 13-17; F, n = 1; G, n =1)

A

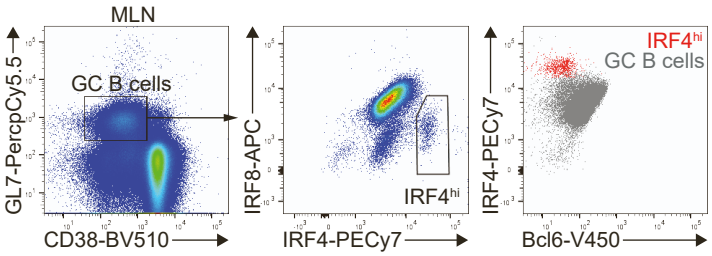

Supplemental Figure 4

Supplemental Figure 4. IRF4^{hi} GC B plasmablast precursors are Bcl6^{lo}. Related to Figure 5.

(A), IRF4, IRF8, and Bcl6 co-staining of mesenteric GC B cells for GC B plasmablast precursors.

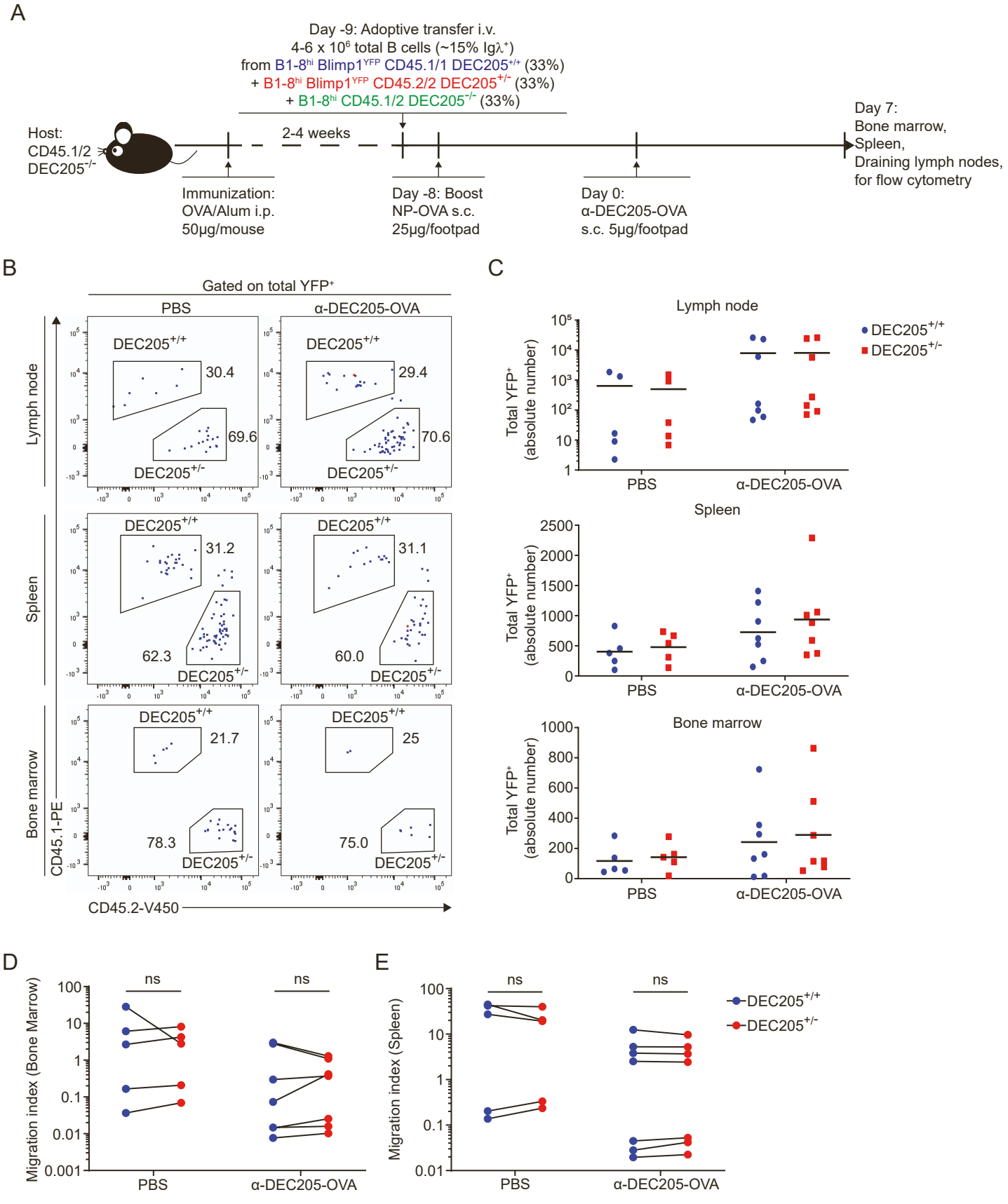

Supplemental Figure 5

Supplemental Figure 5. Migration of plasmablast to bone marrow and spleen are independent of pMHCII density. Related to Figure 6.

(A), Experimental setup for tracking migration of plasmablasts generated from B cells with differential pMHCII density conferred by αDEC-OVA targeting. (B), Representative plot of plasmablasts originated from DEC205$^{+/+}$ and DEC205$^{+/-}$ GC B cells in the draining lymph node, spleen, and bone marrow of mice receiving αDEC-OVA treatment compared to PBS-treated mice. (C), Absolute numbers of DEC205$^{+/+}$ and DEC205$^{+/-}$ plasmablasts in the draining lymph node, spleen, and bone marrow of mice receiving αDEC-OVA treatment compared to PBS-treated mice. (D), Bone marrow/lymph node and (E), spleen/lymph node ratio of plasmablast numbers in mice treated with αDEC-OVA or PBS. All bars show mean. ns, non-significant by paired Student's t test. All graphs show pooled data from at least two independent experiments. (C-E, n = 7)